SahuarUS
Revista electrónica de Matemáticas
Vol. 9 / No. 1 / Julio 2025, pp. 11-33
SahuarUS
REVISTAS UNISON
"El saber de mis hijos hará mi grandeza"

Numerical Simulation of Pollutant Transport in the Rio das Mortes Using Finite Element Methods

André Krindges,[1] Gabriela Scavazini da Silva de Oliveira [2] and João Frederico da Costa Azevedo Meyer[3]
[1]Federal University of Mato Grosso
[2,3]State University of Campinas
[1]andre.krindges@ufmt.br, [2]gscavazini@gmail.com and [3] jmeyer@unicamp.br

Abstract

This study investigates pollutant dispersion in the Rio das Mortes using mathematical modeling based on partial differential equations. The research applies the Finite Element Method (FEM) for spatial discretization and the Crank-Nicolson method for temporal discretization. The Navier-Stokes equation is used to model the river's velocity field, providing a realistic representation of pollutant transport. The study focuses on a specific region in Nova Xavantina, Mato Grosso, where agricultural activities, mining, and tributary streams influence water quality. Two different pollution scenarios are analyzed: (1) a single upstream pollutant source, and (2) multiple pollutant sources, including tributary inputs. The numerical simulations indicate that in the first scenario, pollutant concentration stabilizes after approximately six days, while in the second scenario, stability is reached after 125 days. The results highlight the effectiveness of mathematical modeling in predicting environmental impacts and aiding in pollution management. However, the lack of field data limits the precision of the simulations. Future work should include field sampling to calibrate the model parameters and validate the results. Additionally, developing a computational tool to simulate different pollution scenarios in riverine environments could be beneficial for environmental policy-making. This research underscores the importance of mathematical and computational tools in ecological studies, contributing to sustainable water resource management.

Keywords: Pollutant Dispersion, Finite Element Method, Mathematical Modeling.

DOI: 10.36788/sah.v9i1.161
Recibido: 31 de enero de 2025.
Aceptado: 23 de junio de 2025.

1. Introduction

The continuous advancement of science has brought countless contributions to society, both positive and negative. From the earliest days of humanity to the technological breakthroughs that enabled space exploration, scientific knowledge has progressed significantly. Today, we live in an era defined by rapid technological development, which drives economic

growth and reshapes how we interact with the world. While the benefits of science—such as increased food production, job creation, accelerated vaccine development, and advances in sustainable energy—are widely acknowledged, it is equally important to address the challenges that accompany these advancements. These challenges include environmental pollution, radioactive waste, the consequences of armed conflicts, economic disparities, and other adverse effects that impact both society and nature.

In this context, science and technology play a crucial role in mitigating these negative impacts and fostering the construction and restoration of healthy environments. This study aims to develop mathematical and computational tools to analyze regions affected by pollutant emissions resulting from human activities, such as agriculture, livestock farming, tourism, and mining. These pollutants can contaminate rivers and disrupt the ecosystems they support, leading to significant environmental damage.

To address this issue, the study employs Differential Equations, a fundamental tool for modeling real-world phenomena. As described by [1], the use of differential equations follows essential steps, including data collection, model abstraction, analysis and resolution, result validation, necessary adjustments, and, ultimately, application to similar scenarios. In particular, Partial Differential Equations (PDEs), widely used in fields such as Mathematical Physics and Biomathematics, will serve as the primary analytical tool.

Building on the works of [4], [10], and [12], we conducted a case study on the Rio das Mortes, located in the state of Mato Grosso, to assess the environmental impacts of a specific pollutant in this region.

2. Problem Delimitation

In order to analyze the pollution conditions present in rivers, the location for this study has been defined, and a brief presentation follows. The chosen location is the Rio das Mortes, which originates in the state of Mato Grosso, in the Serra de São Lourenço, in the municipality of Campo Verde. According to [6], it is the most important sub-basin of the Araguaia River, located on the left bank. The river is approximately 1150 km long and hosts a biodiversity typical of the Cerrado region, as shown in Figure 1.

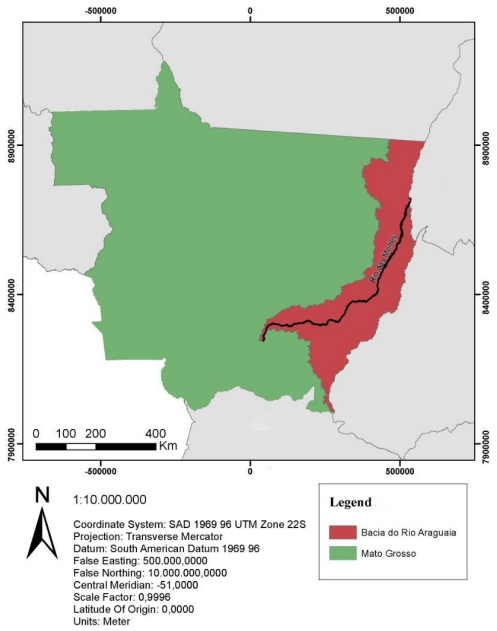

Figure 1: Araguaia River Basin in the State of Mato Grosso.
Source: Gabriela Scavazini and Douglas Castro, 2023

Also known as the Rio Manso, this name is less commonly used. According to [7], the name Rio das Mortes originated during the colonization period, which was marked by conflicts between indigenous peoples and the Bandeirante expeditions. Many deaths occurred, and the bodies were thrown into the river, which then became known as the River of Deaths.

The Rio das Mortes flows through the following municipalities in Mato Grosso: Campo Verde, Poxoréo, Primavera do Leste, Novo São Joaquim, Indianópolis, Nova Xavantina, Nova Nazaré, Cocalinho, and Novo Santo Antônio. Among these, Nova Xavantina is the only municipality directly traversed by the river.. Its main tributaries are: Rio São Marcos, Noidore, Areões, Pindaíba, Borecaia, Água Suja, Pimentel Barbosa, and Corixão.

The decision to study the dispersion of pollutants in this river is important because, according to [7], it is one of the most significant rivers in the state, supplying water to 21 municipalities, 11 of which have economic activities predominantly within the river basin. These activities include farming, livestock, sports, and fishing for the subsistence of indigenous communities and riverside populations.

According to [7], the Rio das Mortes watershed is being affected by indiscriminate deforestation due to agricultural activities. Analysis of testimonies from local residents revealed the need for Environmental Education to raise awareness of the river's importance for the region's activities.

Therefore, it is crucial to investigate the effects of pollutants in the Nova Xavantina region, as the river runs through the city and is highly relevant for local activities. This analysis is important to alert local and state authorities about the potential environmental impacts that pollutants discharged into the river may cause to the ecosystem in the area.

Due to the river's extensive length, the study has been limited to a specific region in the

municipality of Nova Xavantina – MT. In this area, there are agricultural plantations, a gold mine, two streams that flow into the Rio das Mortes (one unnamed and the other called Ribeirão Antártico), and some ranches along the river's banks.

This study is based on research conducted by the Biomath group at IMECC, which has developed studies on pollutant dispersion using the Finite Element Method (FEM) over the years. These studies vary in complexity, from models with constant velocity fields to more advanced analyses, such as the most recent work by [10], which considers time-varying boundaries and the use of Navier-Stokes equations. These contributions provide the mathematical and computational foundation to address the environmental issue being studied.

3. Classical Model

3.1. Advection-diffusion Equation

The analysis of aquatic pollution is crucial to understanding the environmental impacts caused by human activities, such as waste disposal and mining operations. To address this, mathematical models based on the advection-diffusion equation are employed. These models describe the variation in pollutant concentration over time and space, accounting for processes like diffusion, transport, decay, and pollution sources.

The general equation governing the problem is:

$$\frac{\partial C}{\partial t} - \alpha \Delta C + \nabla \cdot \vec{\mathbb{V}} C + \sigma C = f, \forall (x, y) \in \Omega \quad e \quad t \in J = (0, T], \tag{1}$$

where $C(x, y, t)$ represents the pollutant concentration, α is the diffusion coefficient, $\vec{\mathbb{V}}$ is the velocity field (representing water flow), σ is the pollutant decay rate, and f represents source terms, including runoff and direct discharges.

In addition to diffusion and advection, the equation also includes reactive terms that account for phenomena directly affecting the pollutant concentration through chemical, physical, or biological interactions with the environment. In the adopted model, the reactive term is represented by σC, where σ denotes the pollutant decay rate. This term simulates natural processes of deposition or degradation of the pollutant throughout the domain, such as absorption by riverbanks, chemical reactions within the riverbed, or biological degradation of the substance. These processes gradually reduce the pollutant concentration and are therefore essential for realistically representing the pollution dynamics in aquatic environments.

A 3D model would better capture vertical variations in flow and pollutant concentration, including phenomena such as vertical mixing, sedimentation, and stratification, which may be critical in deep or strongly stratified water bodies. The absence of these effects in a 2D model can limit accuracy when vertical gradients are significant. However, the 2D approach remains valid under certain conditions: the water body is relatively shallow compared to its horizontal dimensions, vertical flow components are negligible, and the pollutant is well-mixed in the vertical direction due to turbulence or mechanical mixing. Under these assumptions, the 2D model, which considers depth-averaged concentration, can effectively represent the main

transport and diffusion processes. Thus, the results may be considered reliable for predicting large-scale spatial and temporal pollution patterns in such environments.

Our problem will be analyzed in a two-dimensional setting. Since this involves partial differential equations, it is necessary to define certain conditions, specifically boundary conditions. For this problem, we will use two types of boundary conditions: Von Neumann and Robin. These were chosen because they effectively represent the processes of pollutant input and loss.

To facilitate the identification of each boundary condition, we divide the boundary $\partial\Omega$ into several parts, denoted as $\partial\Omega = \Gamma_1, \Gamma_2, \ldots, \Gamma_{11}$. This division is shown in Figure 2, where the coordinates are presented in terms of latitude and longitude — with the x-axis representing longitude and the y-axis representing latitude.

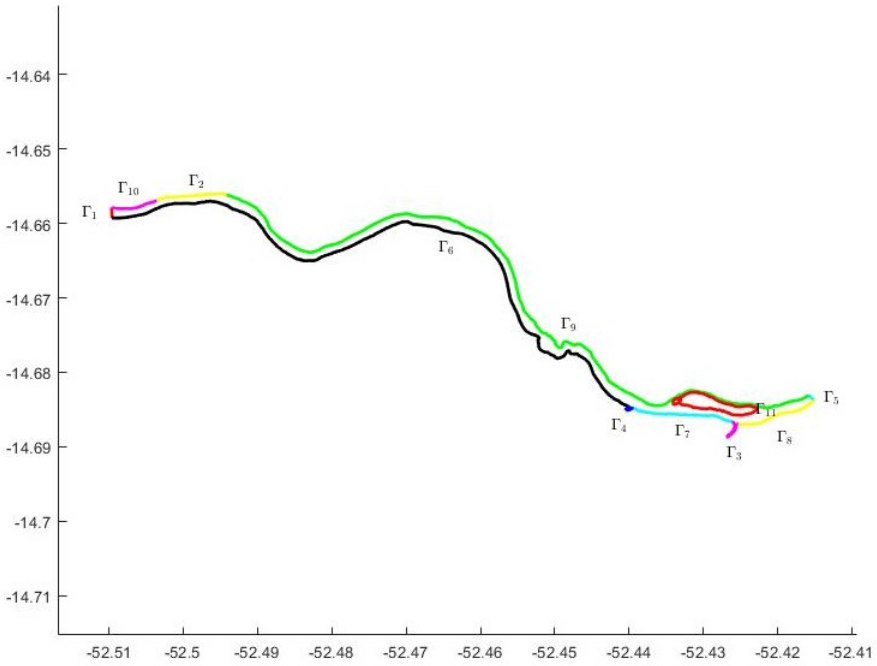

Figure 2: Boundary.
Source: [11]

For cases involving the inflow of pollutants into the aquatic environment, we use the Von Neumann boundary condition. This condition represents the pollutant input, which depends on a function g_m at position (x, y) and time t:

$$\alpha \frac{\partial C}{\partial \eta}\Big|_{\Gamma_m} = g_m \quad \textit{(Von Neumann)},$$

where Γ_1 represents the inflow boundary of the river, and $\Gamma_2, \Gamma_3, \Gamma_4$ represent three pollution sources directly discharging into the river.

In this work, the function g_m is time-dependent and non-negative, representing a variable pollutant input rate at the boundaries $\Gamma_1, \Gamma_2, \Gamma_3$ and Γ_4 This condition reflects pollutant

discharges that may fluctuate over time, mimicking real-world scenarios where contamination levels can vary due to external or operational factors.

For pollutant losses, we employ the Robin boundary condition, where k_m is a constant that controls the rate of pollutant loss. This condition is applied at Γ_5, which represents the river's outflow boundary, and at $\Gamma_6, \Gamma_7, \Gamma_8, \Gamma_9, \Gamma_{10}, \Gamma_{11}$:

$$\alpha \frac{\partial C}{\partial \eta}\Big|_{\Gamma_m} = k_m C \quad \textit{(Robin)}.$$

Physically, the Robin boundary condition represents a proportional relationship between the concentration of pollutants at the boundary and the rate at which they are removed from the system. It is suitable for modeling processes such as dilution, absorption, or natural decay that occur when pollutants reach the riverbanks or exit the domain. In our model, this condition is used along the downstream boundary to simulate the continuous transport of pollutants out of the study area, and along the riverbanks to account for interactions with the surrounding environment, such as infiltration into the soil or uptake by vegetation.

For simplicity, we can rewrite the governing equation for our problem as follows:

$$\begin{cases} \dfrac{\partial C}{\partial t} - \alpha \Delta C + \nabla \cdot \vec{\mathbb{V}} C + \sigma C = f, & \forall (x,y) \in \Omega,\ t \in J = (0,T], \\ \nabla \cdot \vec{\mathbb{V}} = 0, & \textit{(incompressible fluid)}, \\ \alpha \dfrac{\partial C}{\partial \eta}\Big|_{\Gamma_1} = g_1(x,y,t), & t \in J = (0,T], \\ \alpha \dfrac{\partial C}{\partial \eta}\Big|_{\Gamma_2} = g_2(x,y,t), & t \in J = (0,T], \\ \alpha \dfrac{\partial C}{\partial \eta}\Big|_{\Gamma_3} = g_3(x,y,t), & t \in J = (0,T], \\ \alpha \dfrac{\partial C}{\partial \eta}\Big|_{\Gamma_4} = g_4(x,y,t), & t \in J = (0,T], \\ -\alpha \dfrac{\partial C}{\partial \eta}\Big|_{\Gamma_5} = k_5 C, & t \in J = (0,T], \\ -\alpha \dfrac{\partial C}{\partial \eta}\Big|_{\Gamma_6} = k_6 C, & t \in J = (0,T], \\ -\alpha \dfrac{\partial C}{\partial \eta}\Big|_{\Gamma_7} = k_7 C, & t \in J = (0,T], \\ -\alpha \dfrac{\partial C}{\partial \eta}\Big|_{\Gamma_8} = k_8 C, & t \in J = (0,T], \\ -\alpha \dfrac{\partial C}{\partial \eta}\Big|_{\Gamma_9} = k_9 C, & t \in J = (0,T], \\ -\alpha \dfrac{\partial C}{\partial \eta}\Big|_{\Gamma_{10}} = k_{10} C, & t \in J = (0,T], \\ -\alpha \dfrac{\partial C}{\partial \eta}\Big|_{\Gamma_{11}} = k_{11} C, & t \in J = (0,T]. \end{cases} \tag{2}$$

3.2. Navier-Stokes equation

The Navier-Stokes equation is used in fluid mechanics to describe the behavior of Newtonian fluids. A classic example of a Newtonian fluid is water, as its viscosity remains constant regardless of the flow velocity or shear stress. For this reason, we will use this equation to create a velocity field.

By observing the equation (1), we see that the component $\vec{\mathbb{V}}$ is responsible for transporting the pollutant within the water flow. Therefore, following the references [4] and [10], we will construct our velocity field based on a velocity profile defined at the river's entrance.

$$\begin{cases} \dfrac{\partial \vec{\mathbb{V}}}{\partial t} + \left(\vec{\mathbb{V}} \cdot \nabla\right) \vec{\mathbb{V}} + \nabla p - \nu \Delta \vec{\mathbb{V}} = \vec{F}, \forall \ \ (x, y) \in \Omega, t \in J = (0, T], \\ \nabla \cdot \vec{\mathbb{V}} = 0 \ \ \textit{(incompressible fluid)}, \end{cases} \tag{3}$$

where:
$\vec{\mathbb{V}}$: velocity field, in this case, horizontal and vertical;
p: pressure exerted on the fluid;
ν: fluid viscosity, i.e., the friction the fluid has with the medium;
$\vec{F}$: external force field.

Just like in the advection-diffusion equation, it is necessary to define boundary conditions for the Navier-Stokes equation. Consider the following conditions:

- Water inlet: At the river's entrance, we will define the velocity profile of the water. For this, we will use a non-homogeneous Dirichlet boundary condition.
  $\vec{\mathbb{V}}\Big|_{\Gamma_1} = \vec{q}(x, y, t)$, for $(x, y) \in \Omega$ and $t \in J = (0, T]$.
- Water outlet: We will leave the outlet open, so we will use a homogeneous Von Neumann boundary condition because the outgoing vector must be perpendicular to the cross-section made in the river.
  $\dfrac{\partial \vec{u}}{\partial \eta}\Big|_{\Gamma_m} = \dfrac{\partial \vec{v}}{\partial \eta}\Big|_{\Gamma_m} = 0$, with $m = 2, 3, 4, 5, 6, 7, 8, 9, 10$ and 11 and $\vec{\mathbb{V}} = (\vec{u}, \vec{v})$

4. Variational Formulation and Discretization

Variational formulation is a technique used to find approximate solutions to mathematical problems, especially when an exact solution is difficult or impossible to find. It involves transforming the original differential equation into an equivalent problem of finding a function within a specific functional space. Instead of searching for an exact solution, the goal is to find a solution that minimizes an energy-like quantity associated with the problem, using approximation methods such as the Galerkin Method.

For the advection-diffusion equation, the variational formulation aims to transform the differential equation into an expression that involves integrals and inner products, using test functions (denoted by v) to represent the approximate solution. This results in an integral

equation that describes the solution in terms of variables that are easier to manipulate numerically.

The variational formulation of the advection-diffusion equation can be written as follows:

$$\left(\frac{\partial C}{\partial t}|v\right)_\Omega + \alpha(\nabla C|\nabla v)_\Omega + \sum_{m=5}^{11} k_m \left(C|v\right)_{\Gamma_m} + \left(\vec{\mathbb{V}}\cdot\nabla C|v\right)_\Omega + \sigma(C|v)_\Omega = (f|v)_\Omega + \sum_{m=1}^{4}(g_m|v)_{\Gamma_m}$$

In this equation, the integrals represent the variational terms of the original equation, and the boundary conditions are applied appropriately on the domain boundaries. The solution is obtained approximately using methods like the Galerkin Method and temporal discretization with Crank-Nicolson.

The notation $(f|g)_\Omega$ used in this formulation denotes the *inner product* between the functions f and g over the domain Ω, and is defined as

$$(f|g)_\Omega = \int_\Omega f \cdot g \, d\Omega.$$

This notation is equivalent to the more traditional $\langle f, g\rangle$ commonly used in functional analysis.

4.1. Spatial and Temporal Discretization

In this chapter, we address the discretization of the advection-diffusion equation. Starting from the variational formulation, we aim to determine the solution to the problem. Since this scenario may lack an analytical solution, we employ the Galerkin Method to obtain an approximation. For this purpose, we use the finite element method for spatial discretization and the Crank-Nicolson method for temporal discretization.

Spatial discretization via the finite element method involves dividing the solution domain into a finite number of subdomains, referred to as elements, to approximate the problem's solution. Considering Ω as the region containing the equation's results, we divide Ω into a finite number of two-dimensional triangles, ensuring that the union of these elements closely approximates the domain Ω. Denoting $\Omega_h \to \Omega$, as the boundary $\partial\Omega_h$ approaches $\partial\Omega$, greater accuracy of the weak solution is achieved. Mathematically, we consider $\mathcal{V}_h$ as a finite vector subspace of dimension n of $\mathcal{V}$, with the basis $\mathfrak{B}(\mathcal{V}_h) = \{\Phi_1, \Phi_2, \Phi_3, ..., \Phi_n\}$. The solution $C(x, y, t)$ is approximated by $C_h(x, y, t)$, where $C_h(x, y, t) \in \mathcal{V}_h$ is expressed as a linear combination of the basis elements: $C_h(x, y, t) = \sum_{j=1}^{n} c_j(t)\Phi_j(x, y)$.

Substituting $C_h(x, y, t)$ into the variational formulation yields a new equation where the partial derivatives and terms of the original problem are expressed in terms of the basis functions Φ_j. Applying summation properties and considering that $c_j(t)$ depends only on time t, we rewrite the equation in a more compact form. This formulation involves integrals over the domain Ω and the boundary Γ_m, which, when discretized, result in coefficient matrices.

By substituting $C_h(x, y, t)$ into the variational formulation and applying the linearity of integration along with the properties of the basis functions Φ_j, we obtain a system of ordinary

differential equations whose coefficients depend on time. These equations, when written in matrix notation, yield:

$$\frac{\partial c_j(t)}{\partial t} \cdot \mathbb{M} + c_j(t) \cdot \mathbb{P} = \mathbb{B},$$

as presented on the following page. This matrix equation is directly derived from the spatial discretization of the advection-diffusion equation using the finite element method and corresponds to the weak form projected onto the finite-dimensional subspace $\mathcal{V}_h$. Thus, the matrix formulation shown is a discrete representation of the previously discussed advection-diffusion equation.The terms presented have the following representation: $\mathbb{M}$ is the mass matrix, $\mathbb{P}$ is the stiffness matrix containing the terms associated with diffusion, boundary conditions, and reaction coefficients, and $\mathbb{B}$ is the force vector associated with source terms. To separately handle the advection, the matrix $\mathbb{P}$ is divided into two parts: $\mathbb{P}$, containing the diffusion and reaction terms, and $\mathbb{Q}$, which includes the advective terms. Thus, the equation is rewritten as:

$$\frac{\partial c_j(t)}{\partial t} \cdot \mathbb{M} + c_j(t) \cdot (\mathbb{P} + \mathbb{Q}) = \mathbb{B}.$$

With spatial discretization completed, we proceed to temporal discretization. In this context, we utilize different time integration methods, such as the explicit Euler method, the implicit Euler method, and the Crank-Nicolson method. Each method has specific characteristics in terms of stability and accuracy, with Crank-Nicolson chosen for its unconditional convergence and error of order $(\Delta t)^2$.

Thus, the discretization process, both spatial and temporal, enables the approximate solution of the advection-diffusion equation, providing numerical results that can be refined according to the selected element mesh and time step.

4.2. Temporal Discretization

To perform temporal approximation, we can use three methods:

- Explicit Euler method: conditional convergence and error of order Δt;
- Implicit Euler method: unconditional convergence and error of order Δt;
- Crank-Nicolson method: unconditional convergence and error of order Δt^2.

Considering convergence and error order, the ideal method for temporal discretization is Crank-Nicolson, which approximates the derivative at the midpoint, i.e., $t_{n+\frac{1}{2}} = t_{n+}\frac{\Delta t}{2}$. According to [3], despite its numerical instability at the beginning, it stabilizes after a few iterations, achieving a curve that best fits the problem.

Thus, we have the following numerical approximations:

$$\begin{aligned} \left.\frac{\partial c_j(t)}{\partial t}\right|_{t_{n+\frac{1}{2}}} &\cong \frac{{c_j}^{n+1} - {c_j}^n}{\Delta t}, \qquad \left. c_j(t)\right|_{t_{n+\frac{1}{2}}} \cong \frac{{c_j}^{n+1} - {c_j}^n}{2}, \\ \left.\mathbb{Q}\right|_{t_{n+\frac{1}{2}}} &= \frac{\mathbb{Q}^{n+1} + \mathbb{Q}^n}{2}, \qquad \left. g_m\right|_{t_{n+\frac{1}{2}}} = \frac{g_m^{n+1} + g_m^n}{2} \end{aligned} \tag{4}$$

Rewriting, we obtain:

$$\frac{{c_j}^{n+1} - {c_j}^n}{\Delta t} \cdot \mathbb{M} + \frac{{c_j}^{n+1} - {c_j}^n}{2} \cdot \mathbb{P} + \frac{{c_j}^{n+1} - {c_j}^n}{2} \left(\frac{\mathbb{Q}^{n+1} + \mathbb{Q}^n}{2} \right) = \mathbb{B}^{n+\frac{1}{2}}$$

By multiplying all terms by Δt and making some adjustments, we get:

$$\begin{aligned} &\left(\mathbb{M} + \frac{\Delta t}{2}\mathbb{P} + \frac{\Delta t}{2} \left(\frac{\mathbb{Q}^{n+1} + \mathbb{Q}^n}{2} \right) \right) C_j^{n+1} = \\ &\left(\mathbb{M} + \frac{\Delta t}{2}\mathbb{P} + \frac{\Delta t}{2} \left(\frac{\mathbb{Q}^{n+1} + \mathbb{Q}^n}{2} \right) \right) C_j^n + \Delta t \cdot \mathbb{B}^{n+\frac{1}{2}}, \end{aligned} \tag{5}$$

Thus, we construct the discretization concerning space and time. Now let us analyze the numerical results.

5. Numerical Results

Although there are no specific experimental data available for the direct validation of this study, the initial conditions were defined based on data from previous experiments conducted in scenarios very similar to the one analyzed here. These data were obtained from the works of [3], [4], [10], [12]. The selection of these parameters was supported by the physical and operational similarities between those studies and the current context, providing a realistic and consistent basis for the simulations.

6. Domain Discretization and Inflow Velocity Profile

To construct the results, we must first discretize our domain, that is, divide it into a finite number of elements and, from there, begin the implementation to obtain results.

According to [5], [8] and [9], the finite element method (FEM) consists of dividing the problem domain into a mesh or network of smaller and simpler elements, such as triangles or tetrahedra in the case of two-dimensional and three-dimensional problems, respectively. Each element is characterized by a series of physical properties and is associated with a mathematical approximation function, known as a shape function. These shape functions are used to represent the behavior of the problem within each element. For this specific problem, we will use triangular and two-dimensional elements.

The mesh was constructed using GMSH software, with elements oriented in a counter-clockwise direction.. This is a free and open-source software used for mesh generation in numerical simulations and computational modeling. It is widely used in the field of numerical methods, especially in the context of the finite element method. It is worth noting that all the following plots are presented in UTM coordinates, which represent a cartographic projection system widely used in geographic applications. This system divides the Earth's surface into zones and provides coordinates in meters, making it easier to work with distances and areas in spatial simulations.

To ensure the transparency and reproducibility of the numerical results, the computational system used for the implementation consisted of a computer equipped with two 6-core Xeon processors, 144 GB of RAM, and the Windows operating system. The implementation was carried out using MATLAB R12 (also known as MATLAB 6.0) and included explicit parallelization to optimize processing time.

The use of parallelization significantly reduced the time required for each simulation, which ranged from 15 to 18 hours depending on the mesh complexity and the number of iterations needed for convergence.

This characterization of the computational environment and performance is essential to contextualize the obtained results and to allow comparisons with other implementations.

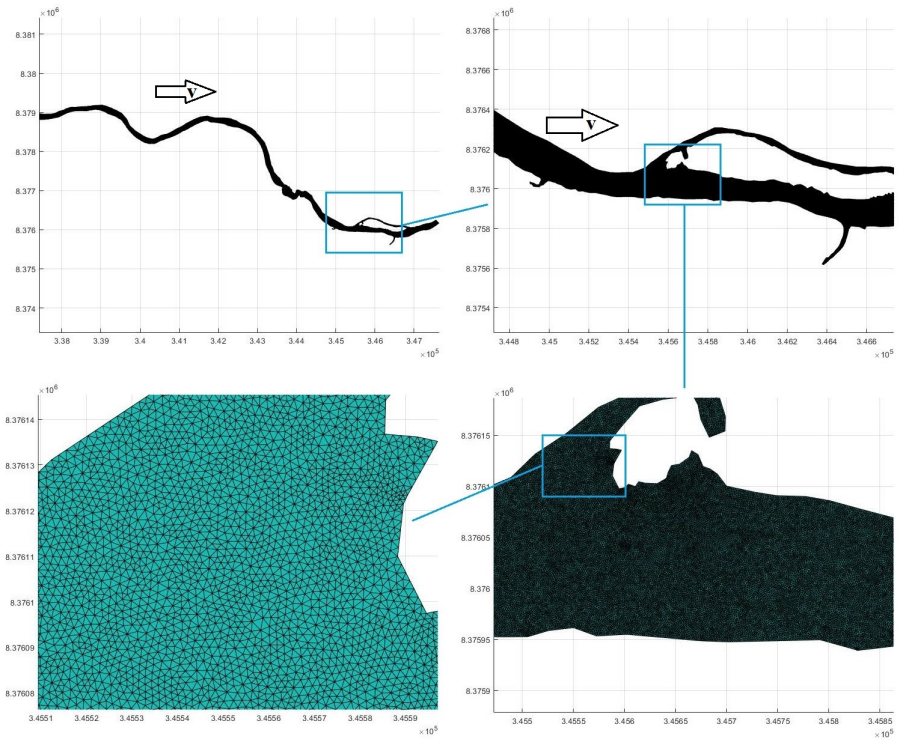

Figure 3: Enlarged mesh.
Source: [11]

- Number of nodes: $592,477$
- Number of elements: $1,170,230$
- Number of boundary elements: $14,724$

Once the domain has been discretized with finite elements, boundary conditions, which were presented in section 3, are established, and the system of equations governing the problem is formulated. The resulting system of equations is generally a set of linear algebraic

equations, which are solved numerically using techniques such as the Gaussian elimination method or iterative methods like the Jacobi or Gauss-Seidel method.

After discretizing the mesh, we proceed to construct the inflow velocity profile of the river. Using the Navier-Stokes equation, we establish the velocity profile of the river and then apply it to the advection-diffusion equation. It is important to note that, depending on the flow regime and boundary conditions, the velocity profile $\mathbf{V}(x,t)$ may reach a steady-state behavior, effectively becoming time-independent and represented as $\mathbf{V}(x)$. However, in more complex scenarios, temporal variations or transient behaviors could be captured, reflecting dynamic flow conditions.

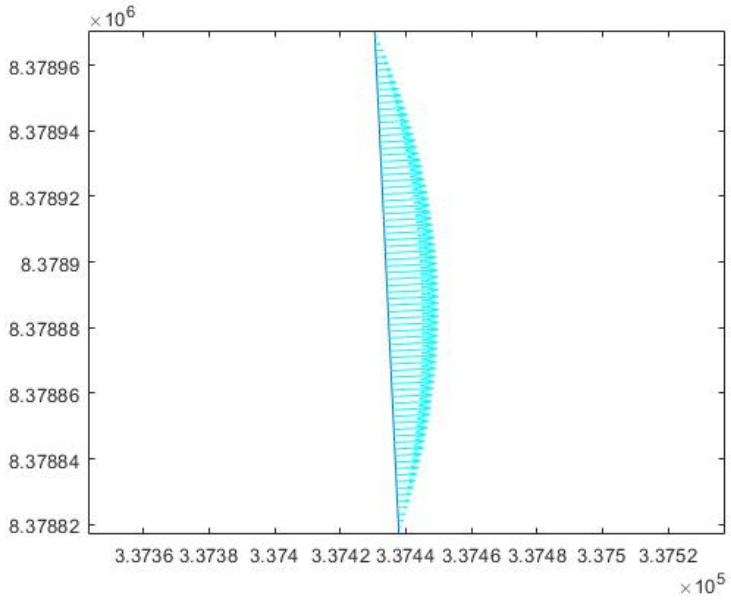

Figure 4: Rotated inflow velocity profile of the Rio das Mortes.
Source: [11]

Figure 4 illustrates the parabolic profile inserted at the river's inlet cross-section. This inlet boundary is denoted by Γ_1, where a Dirichlet boundary condition is imposed for the velocity field $\mathbf{V}$. The parabolic profile was obtained by fitting a parabola to the inflow data, resulting in the following function:

$$f(x) = -2.9080 \times 10^{-4} \cdot x(x - 153.4142), \tag{6}$$

which models the magnitude of the velocity at the inlet. Using this function and the Navier-Stokes equations, we constructed the entire velocity field throughout the studied domain. In Figure 5, we can also observe that the greater the water flow, the higher the velocities described by the vectors. Upon observing the enlarged section of the figure, we notice almost non-existent velocities in the upper right corner. This indicates that the water flow is not as intense due to the river's geomorphology, and locations appear where the water course is calmer, also known as "recirculation zones."

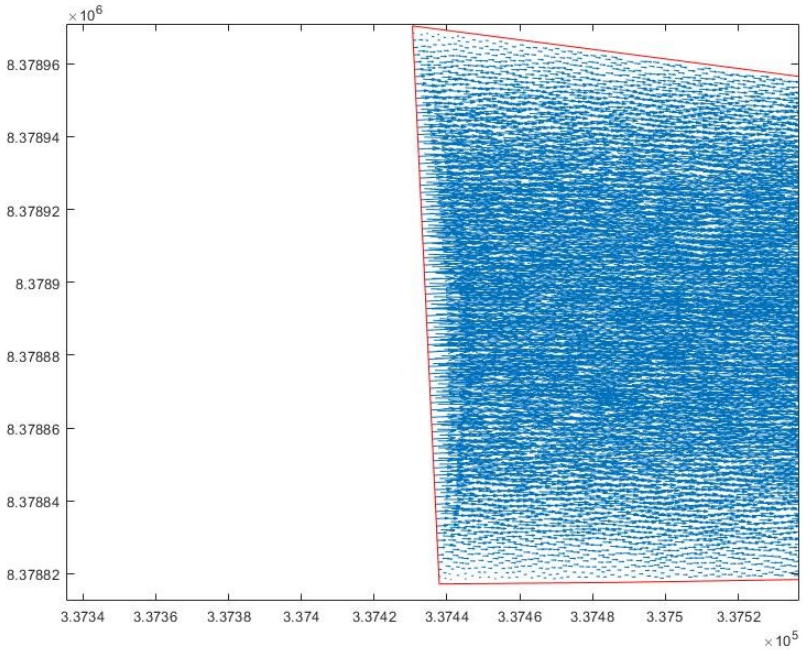

Figure 5: Domain inlet with velocity field.
Source: [11]

7. Analysis and Construction of Results

To implement the code using the finite element method, it is necessary to perform calculations on a reference element and then find the solution for the element under study, as shown in Figure 6 below:

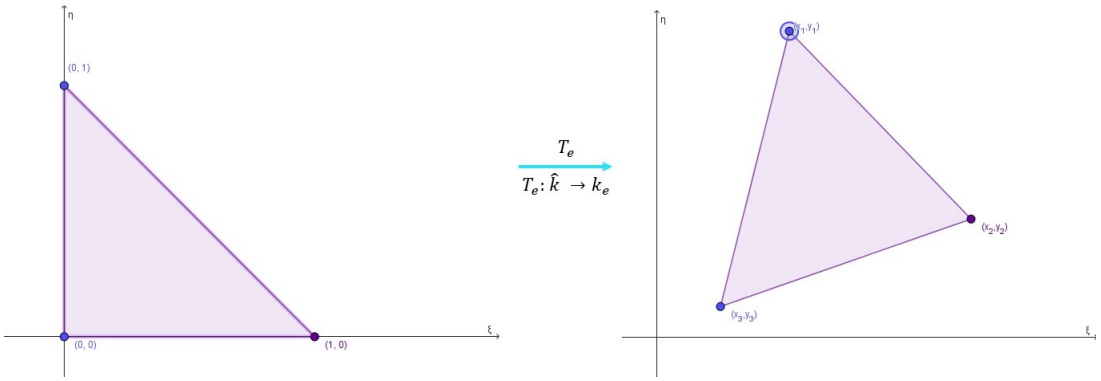

Figure 6: Affine transformation.

The code used for implementation is primarily based on [10]. Through some adaptations

— available at [2] — it was possible to create scenarios to analyze the behavior of a pollutant in the Rio das Mortes. It is important to note that the parameter data are heuristic, as no materials have been collected so far.

For future use of the code, some information must be included. The mesh was constructed counterclockwise, and the coordinates are in kilometers. The velocity fields of the three rivers (Rio das Mortes, Ribeirão Antártico, and the stream) are measured in km/day and remain the same regardless of the scenario used. In these experiments, we consider that the boundary does not vary over time, meaning the river neither floods nor recedes but maintains a constant water level.

All the graphs presented in this work use a Cartesian coordinate system, where the x and y axes represent the UTM (Universal Transverse Mercator) coordinates, converted into a two-dimensional plane. The unit of measurement used in the color maps (Figures 8 to 16) is kilometers per day (km/day), corresponding to the magnitude of the transport or flow being visualized. The choice of measurement units in km/day is due to the fact that, during the resolution of the linear system, using coordinate data in meters would lead to very large numbers, which could cause rounding errors when solving the system. Therefore, it is preferable to work with larger measurement units, in this case, kilometers per day.

Table 1 presents two scenarios, followed by an evaluation of the graphical results obtained. The Reynolds number (Re) was set to 100 based on preliminary tests and references found in the literature. We observed that this value of Re provides a good balance between numerical stability and a physically accurate representation of the studied flow. The other parameters were also obtained from previous studies, ensuring consistency with cases already validated in the literature, as described in the table below.

Table 1: Scenario parameters.

Parameters	Scenario 1	Scenario 2	Unit
Δt	$0,05$	$0,05$	time step
α	$0,2$	$0,2$	km^2/day
σ	24×10^{-4}	24×10^{-4}	$1/day$
g_1	0	24×10^{-12}	km/day
g_2	24×10^{-3}	24×10^{-3}	km/day
g_3	0	24×10^{-6}	km/day
g_4	0	24×10^{-6}	km/day
k_5	0	24×10^{-5}	km/day
k_6	0	24×10^{-5}	km/day
k_7	0	24×10^{-5}	km/day
k_8	0	0	km/day
k_9	0	24×10^{-5}	km/day
k_{10}	0	24×10^{-5}	km/day
k_{11}	0	24×10^{-5}	km/day
Re	100	100	-

To analyze these scenarios, we selected four points in the river, which will serve as support to analyze the stability of the pollutant. In other words, with these points, it is possible to verify that after a certain number of iterations, the graph stabilizes, meaning we have found the numerical approximate solution for the chosen scenario. Figure 7, shown below, presents the points used in this numerical stability test.

It is important to clarify that, in this context, stability refers to numerical stability — that is, the behavior of the numerical solution over time, which becomes consistent and free from oscillations or divergences as the simulation progresses. This does not imply a physically steady state of the river, but rather that the finite element method used is numerically stable and capable of producing reliable approximations after a certain number of iterations.

To ensure numerical stability, some strategies must be considered. One important approach is analyzing the Péclet number (Pe), a dimensionless quantity used to evaluate the balance between convective and diffusive transport in the system. When $Pe \leq 2$, stability is typically maintained. A well-refined mesh also contributes to stability, although it increases computational cost. In this study, we rely on the computational resources of the Federal University of Mato Grosso, with the support of Professor Dr. André Krindges, to obtain stable and accurate solutions using refined meshes while keeping the Péclet condition in mind.

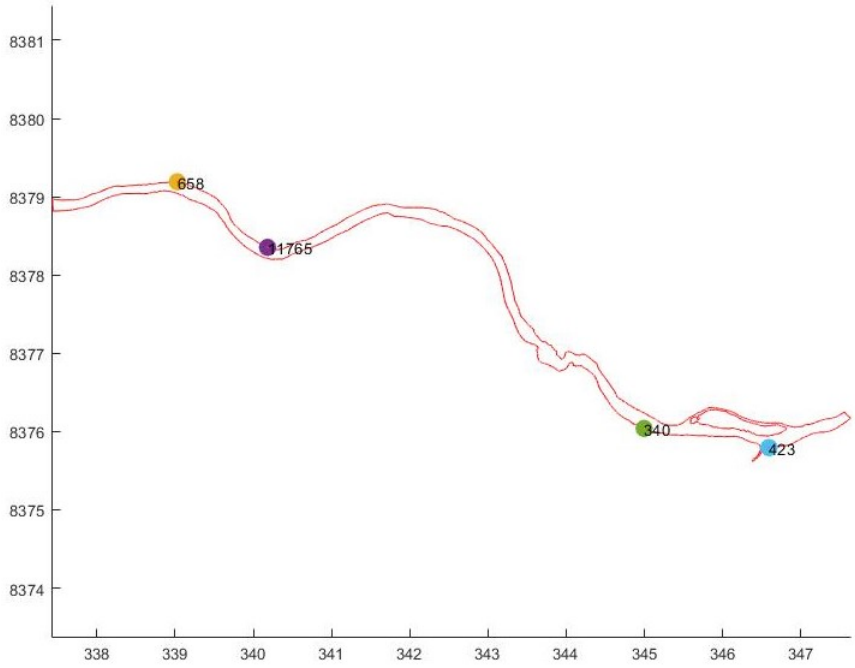

Figure 7: Selected points for analysis.
Source: [11]

The choice of points is motivated by specific hydrological and anthropogenic factors. The yellow point (node 858) was selected due to its proximity to the mining area, making it essential for evaluating the direct influence of mining activities on water quality. The purple

point (node 1165), located upstream of the mining site, was chosen as a reference to represent the natural conditions of the river before any anthropogenic impact. The green point (node 840) and the blue point (node 823) were selected because they are located at the mouths of two tributaries that discharge into the Rio das Mortes. These points are important for assessing the potential contribution of inflows to pollutant dispersion and changes in flow dynamics.

In this first scenario, we simulated a case where the only source of pollution originates from the upstream mining discharge, with all other source terms set to zero. The simulation ran for 3000 iterations; however, each iteration corresponds to a time step of $\Delta t = 0.05$, so 120 iterations amount to approximately 6 days. After this period, the system reaches a numerical steady state, where the concentration of the pollutant no longer changes significantly over time.

It is important to note that the initial peaks observed in Figure 8 represent the transient behavior of the system, which is common in simulations starting from an initial condition far from equilibrium. These values are not numerical errors but reflect the adjustment process of the solution until it stabilizes. The model is stable, and after the transient phase, it converges to a reliable approximation of the stationary solution for the chosen scenario.

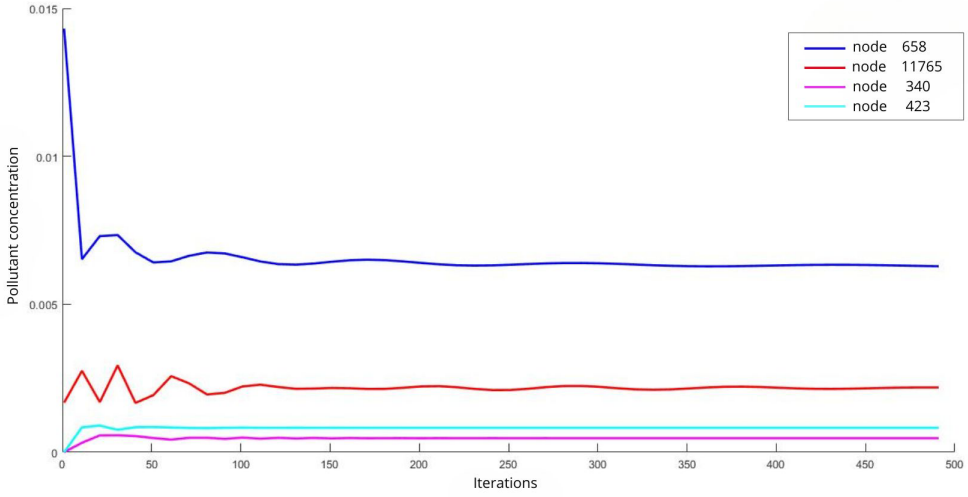

Figure 8: Pollutant concentration over time for scenario 1.
Source: [11]

Figure 9 illustrates the development of pollution over 150 days, while Figure 10 represents the pollution levels at the first and last iterations.

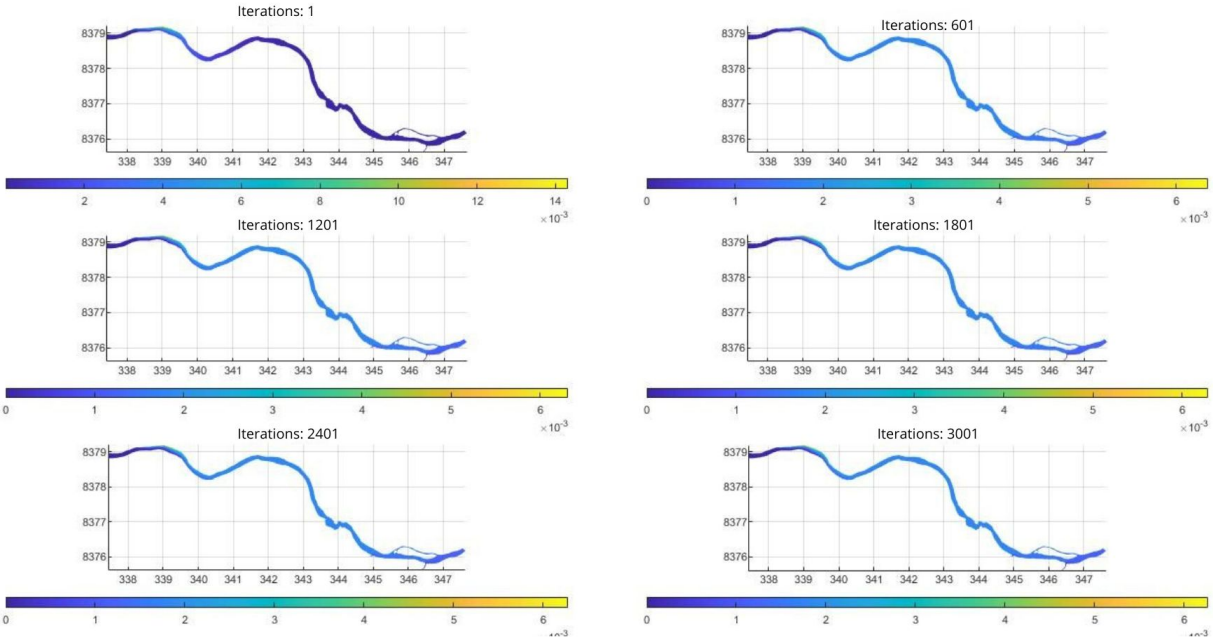

Figure 9: Scenario 1: 150 days.
Source: [11]

¡

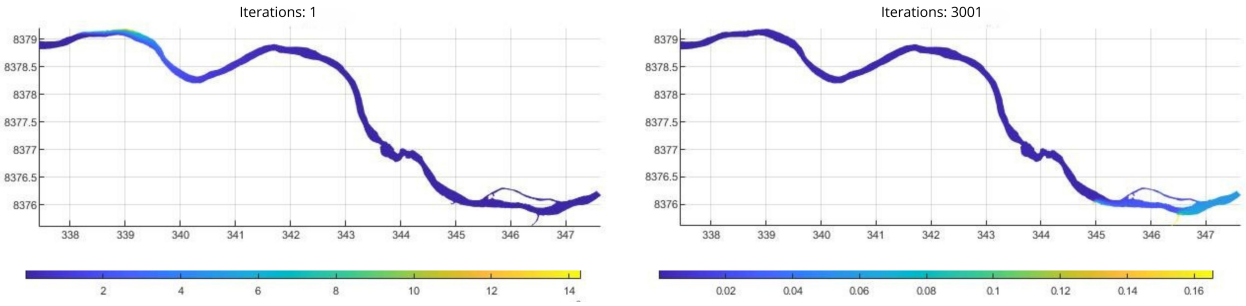

Figure 10: Scenario 1: initial and final pollution.
Source: [11]

In Figure 11, we have a zoomed-in image of the mining region after 150 days of effective pollution.

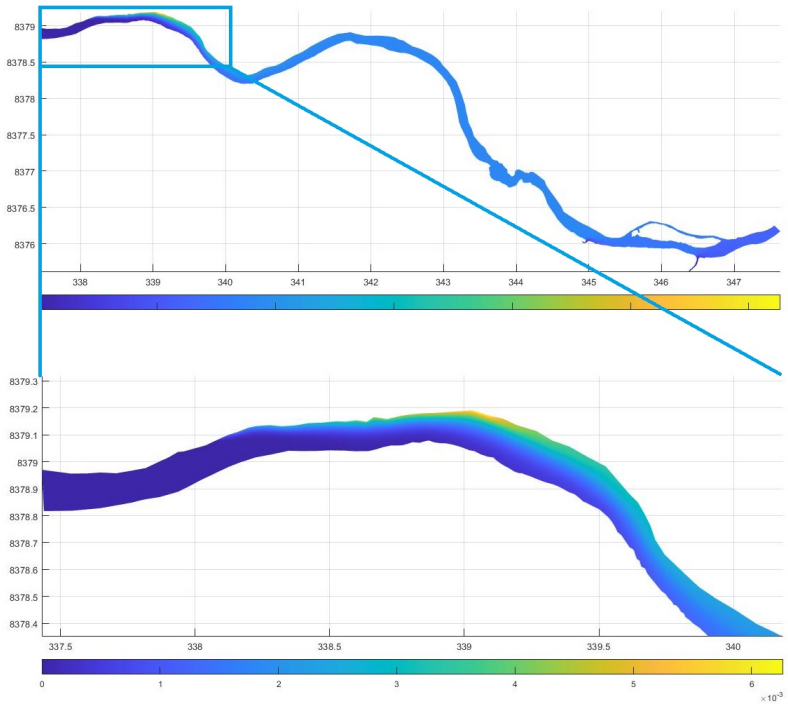

Figure 11: Scenario 1: focus on the mining region.
Source: [11]

Using the data from 1, we now present scenario 2, where the pollutant is applied in the mining area, the creek, and the Antartica stream. Between the Antártica stream and the river outlet, there is the boundary condition k_8, which we consider equal to 0. This value is set to zero to represent a no-loss condition in that final stretch of the river, assuming that there are no significant physical, chemical, or biological processes removing the pollutant before it exits the domain. In other boundary conditions, we set a low pollutant loss and analyzed the result after 3000 iterations. Figure 12 shows the pollutant concentration over time, with numerical stability achieved after 2500 iterations, equivalent to 125 days.

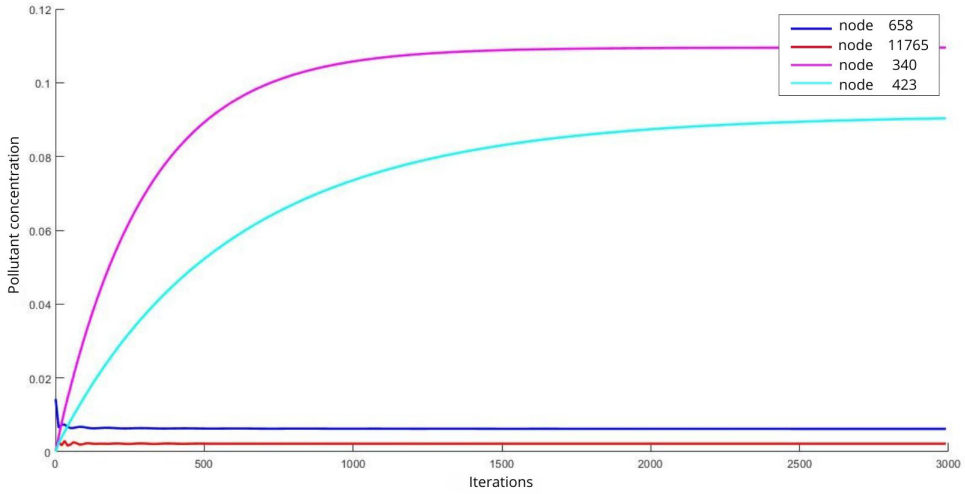

Figure 12: Pollutant concentration over time for scenario 2.

Figures 13 and 14 show the evolution of the pollutant over 150 days. It is worth noting that in this case, the stability of the pollutant concentration can only be seen in the last two images of Figure 13.

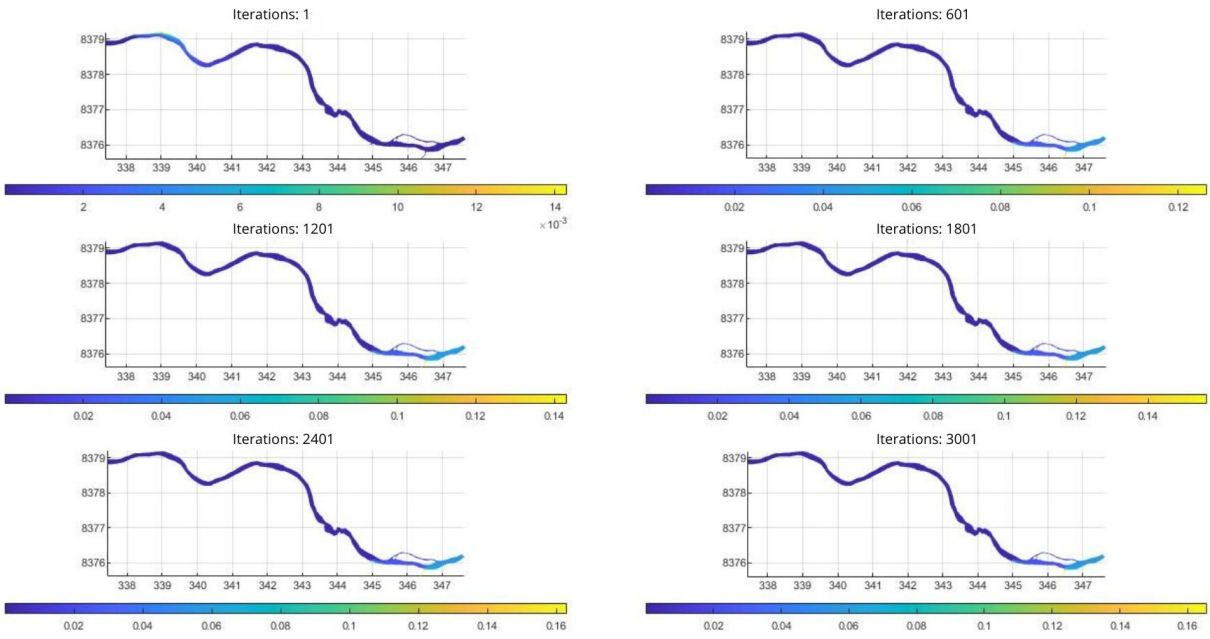

Figure 13: Scenario 2: 150 days.
Source: [11]

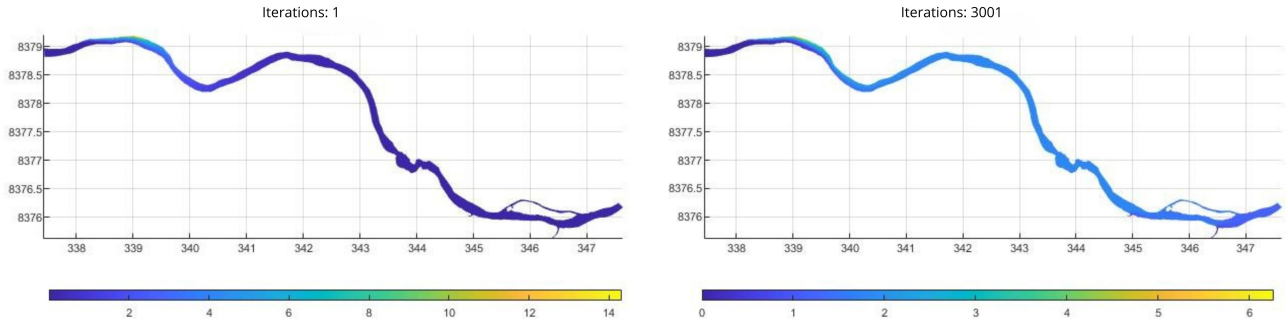

Figure 14: Scenario 2: initial and final pollution.
Source: [11]

Figures 15 and 16 highlight the island region, with the first showing the small island and how the pollutant behaves in that area. The second focuses on the creek and the Antártica stream. In these, it is possible to observe how the pollutant enters the river through the streams, which is caused by the velocity field.

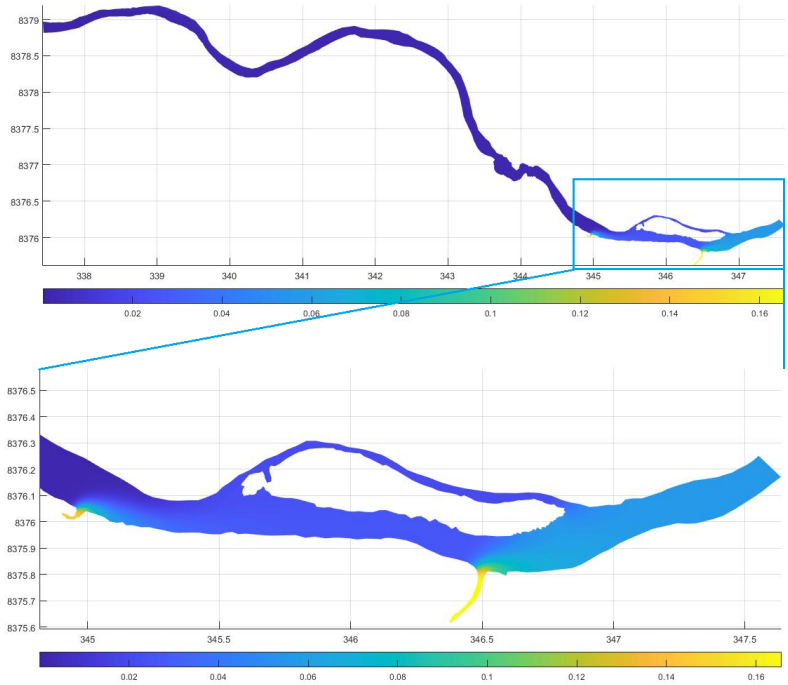

Figure 15: Scenario 2: focus on the island region.
Source: [11]

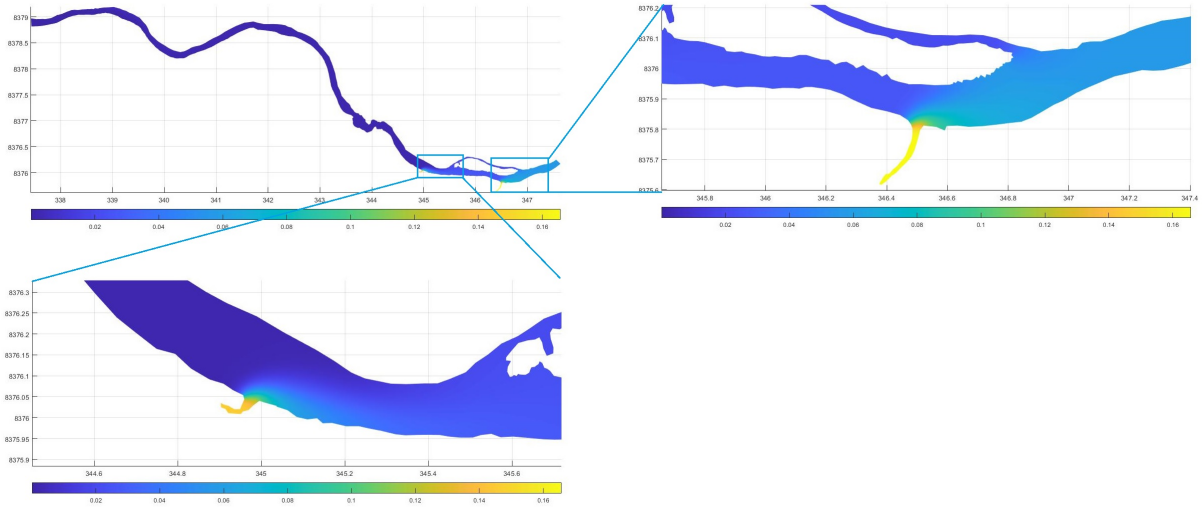

Figure 16: Scenario 2: Focus on the creek and the Antártica stream.
Source: [11]

8. Final Considerations

The study conducted on the Rio das Mortes identified the presence of a pollutant, although it was not specified due to the lack of data on toxic substances in the region. The analysis showed how a pollutant would behave if discharged into the river, and the results were satisfactory, with both the Navier-Stokes and advection-diffusion equations effectively describing the pollutant dispersion. However, factors such as the hydrodynamic characteristics of the river, local weather conditions, and the interaction with aquatic flora and fauna should be considered in future analyses.

In the computational implementation, MATLAB was chosen due to its familiarity, ease of use, and integrated tools for matrix manipulation and data visualization, which facilitated rapid development in this exploratory academic context. Nevertheless, free and robust alternatives such as FEniCSx and deal.II offer promising capabilities for Finite Element Method simulations. A systematic comparison of these platforms, focusing on computational performance, flexibility, and accuracy, would be a valuable contribution and is planned as future work.

Due to the lack of specific parameters, it is essential to conduct field studies to establish these values and improve the understanding of the pollutant dispersion dynamics in the river. Future work could include data collection in different regions of the river to identify critical points and develop mitigation strategies. Additionally, creating a general computational program that handles different pollutant dispersion scenarios in riverine or coastal environments would be a significant advancement for future studies.

The addition of a temporal factor to the model, considering seasonal variations, is also suggested to simulate rivers with periodic width fluctuations. This study is highly relevant in

ecology, as it provides valuable insights into the impact of pollution on aquatic ecosystems, aiding in the preservation and sustainable management of water resources.

Finally, public awareness regarding river pollution and the dissemination of results are crucial to promote collective action and more effective environmental policies.

Acknowledgements

We would like to thank the Brazilian Coordination for the Improvement of Higher Education Personnel (CAPES) – Funding Code 001, for the support granted for the development of this work. This study was partially conducted within the course "Topics in Mathematical Modeling" and was supervised by Dr. João Frederico da Costa Azevedo Meyer, to whom we also express our sincere gratitude. We additionally extend our thanks to our co-supervisor André Krindges, whose support was essential to the completion of this research.

References

[1] R. C. Bassanezi and W. C. Ferreira Jr., *Equações Diferenciais com Aplicações*. S. Paulo: Harbra, 1988.

[2] G. S. S. de Oliveira, "Dissertação - repositório github," https://github.com/gscavazini/dissertacao, 2025, acesso em: 26 jun. 2025.

[3] G. L. Diniz, "Dispersão de poluentes num sistema ar-água: modelagem, aproximação e aplicações," Ph.D. dissertation, FEEC-Unicamp, Campinas/SP, 2003. [Online]. Available: https://doi.org/10.47749/T/UNICAMP.2003.281869

[4] A. Krindges, "Modelagem e simulação computacional de um problema tridimensional de difusão-advecção com uso de navier-stokes," Ph.D. dissertation, IMECC-Unicamp, Campinas/SP, 2011. [Online]. Available: https://doi.org/10.47749/T/UNICAMP.2011.806186

[5] G. I. Marchuk, *Mathematical models in environmental problems: studies in mathematics and its applications*. Netherlands: North-Holland, 1986.

[6] T. L. Melo, F. L.Tejerina-Garro, and C. E. Melo, "Diversidade biológica da comunidade de peixes no baixo rio das mortes, mato grosso, brasil," *Revista Brasileira de Zoologia*, vol. 24, pp. 657–665, 2007. DOI: 10.1590/S0101-81752007000300017

[7] P. M. M. Nápolis, "Políticas públicas na bacia hidrográfica do rio das mortes mato grosso-brasil: Educação ambiental para vidas," Ph.D. dissertation, CCBS-UFSCar, S. Carlos/SP, 2010. [Online]. Available: https://repositorio.ufscar.br/bitstreams/7f66b90f-0709-417e-81fb-86502785dbb0/download

[8] J. T. Oden, E. B. Backer, and G. F. Carey, *Finite Elements an Introduction*. New Jersey: Prentice-Hall, 1981, vol. 1.

[9] A. Okubo, *Diffusion and Ecological Problems: Mathematical Models*. New York: Springer, 1980.

[10] G. S. Silva, "Modelagem, aproximação numérica e simulação computacional de impacto ambiental em meio fluvial: o rio tocantins no município de imperatriz (ma)," Ph.D. dissertation, IMECC-Unicamp, Campinas/SP, 2022. [Online]. Available: https://repositorio.unicamp.br/Busca/Download?codigoArquivo=552701&tipoMidia=0

[11] The MathWorks Inc., *MATLAB version: 9.13.0 (R2022b)*, The MathWorks Inc., Natick, Massachusetts, 2022, software.

[12] L. D. Wolmuth, "Modelagem e simulação do comportamento evolutivo de poluentes em corpos aquáticos de grande extensão: o caso da represa do rio manso," Master's thesis, IMECC-Unicamp, Campinas/SP, 2009. [Online]. Available: https://doi.org/10.47749/T/UNICAMP.2009.470279

Como citar este artículo: G. Scavazini da Silva de Oliveira, A. Krindges, & J. F. da Costa Azevedo Meyer, "Numerical Simulation of Pollutant Transport in the Rio das Mortes Using Finite Element Methods", SahuarUS. Revista Electrónica de Matemática, vol. 9, no. 1, pp. 11–33, 2025. https://doi.org/10.36788/sah.v9i1.161